

2011

## In the heat of the night - alternative pathway respiration drives thermogenesis in *Philodendron bipinnatifidum*

Rebecca Miller

N. Grant

L. Giles

Miquel Ribas-Carbo

J. A. Berry

*See next page for additional authors*

Follow this and additional works at: <https://ro.uow.edu.au/scipapers>



Part of the [Life Sciences Commons](#), [Physical Sciences and Mathematics Commons](#), and the [Social and Behavioral Sciences Commons](#)

---

### Recommended Citation

Miller, Rebecca; Grant, N.; Giles, L.; Ribas-Carbo, Miquel; Berry, J. A.; Watling, Jennifer; and Robinson, Sharon A.: In the heat of the night - alternative pathway respiration drives thermogenesis in *Philodendron bipinnatifidum* 2011.  
<https://ro.uow.edu.au/scipapers/5241>

---

## In the heat of the night - alternative pathway respiration drives thermogenesis in *Philodendron bipinnatifidum*

### Abstract

*Philodendron bipinnatifidum* inflorescences heat up to 42°C and thermoregulate. We investigated whether they generate heat via the cytochrome oxidase pathway uncoupled by uncoupling proteins (pUCPs), or the alternative oxidase (AOX). Contribution of AOX and pUCPs to heating in fertile (FM) and sterile (SM) male florets was determined using a combination of oxygen isotope discrimination, protein and substrate analyses. FM and SM florets thermoregulated independently for up to 30h ex planta. In both floret types, AOX contributed more than 90% of respiratory flux during peak heating. AOX protein increased 5-fold with the onset of thermogenesis in both floret types, whereas pUCP remained low throughout development. These data indicate that AOX is primarily responsible for heating, despite FM and SM florets potentially using different substrates, carbohydrates and lipids, respectively. Measurements of discrimination between O<sub>2</sub> isotopes in strongly respiring SM florets were affected by diffusion; however, this diffusional limitation was largely overcome using elevated O<sub>2</sub>. The first in vivo respiratory flux measurements in an arum show AOX contributes the bulk of heating in *P. bipinnatifidum*. Fine scale regulation of AOX activity is post translational. We also demonstrate that elevated O<sub>2</sub> can aid measurement of respiratory pathway fluxes in dense tissues.

### Disciplines

Life Sciences | Physical Sciences and Mathematics | Social and Behavioral Sciences

### Publication Details

Miller, R. E., Grant, N. M., Giles, L., Ribas-Carbo, M., Berry, J., Watling, J. R. & Robinson, S. A. (2011). In the heat of the night - alternative pathway respiration drives thermogenesis in *Philodendron bipinnatifidum*. *New Phytologist*, 189 (4), 1013-1026.

### Authors

Rebecca Miller, N. Grant, L. Giles, Miquel Ribas-Carbo, J. A. Berry, Jennifer Watling, and Sharon A. Robinson

1 **In the heat of the night – alternative pathway respiration drives thermogenesis**  
2 **in *Philodendron bipinnatifidum***

3 Running title: Alternative oxidase heats *Philodendron*

4  
5 Rebecca E Miller<sup>1,2,3</sup>, Nicole M Grant<sup>1,2</sup>, Larry Giles<sup>4</sup>, Miquel Ribas-Carbo<sup>5</sup> Joseph A Berry<sup>4</sup>,  
6 Jennifer R Watling<sup>2</sup> and Sharon A Robinson<sup>1</sup>

7  
8 <sup>1</sup> *Institute for Conservation Biology and Environmental Management, The University of*  
9 *Wollongong, Wollongong, NSW, 2522, Australia*

10 <sup>2</sup> *Ecology & Evolutionary Biology, School of Earth and Environmental Sciences, The University*  
11 *of Adelaide, Adelaide, SA, 5005, Australia*

12 <sup>3</sup> *School of Biological Sciences, Monash University, Clayton, Victoria, 3800, Australia*

13 <sup>4</sup> *Department of Global Ecology, Carnegie Institution of Washington, 260 Panama St, Stanford,*  
14 *CA 94305, USA*

15 <sup>5</sup> *Universitat de les Illes Balears, Departament de Biologia, Unitat de Fisiologia Vegetal, Illes*  
16 *Balears, Spain*

17 Corresponding author: Rebecca E Miller, School of Biological Sciences, Monash University,  
18 Clayton, Victoria 3800, Australia. Ph. +61 3 99055217, Email: [Rebecca.miller@monash.edu](mailto:Rebecca.miller@monash.edu)

19  
20  
21 **Word count:**

- 22 • Body of text: 6500
- 23 • Introduction: 924
- 24 • Materials & Methods: 1550
- 25 • Results: 1974
- 26 • Discussion: 1966
- 27 • Acknowledgments: 86
- 28 • Tables: 2
- 29 • Figures: 6

## 30 **Summary**

- 31 • *Philodendron bipinnatifidum* inflorescences heat up to 42°C and thermoregulate. We  
32 investigated whether they generate heat via the cytochrome oxidase pathway uncoupled  
33 by uncoupling proteins (pUCPs), or the alternative oxidase (AOX).
- 34 • Contribution of AOX and pUCPs to heating in fertile (FM) and sterile (SM) male florets  
35 was determined using a combination of oxygen isotope discrimination, protein and  
36 substrate analyses.
- 37 • FM and SM florets thermoregulated independently for up to 30h *ex planta*. In both floret  
38 types, AOX contributed more than 90% of respiratory flux during peak heating. AOX  
39 protein increased 5-fold with the onset of thermogenesis in both floret types, whereas  
40 pUCP remained low throughout development. These data indicate that AOX is primarily  
41 responsible for heating, despite FM and SM florets potentially using different substrates,  
42 carbohydrates and lipids, respectively. Measurements of discrimination between O<sub>2</sub>  
43 isotopes in strongly respiring SM florets were affected by diffusion; however, this  
44 diffusional limitation was largely overcome using elevated O<sub>2</sub>.
- 45 • The first *in vivo* respiratory flux measurements in an arum show AOX contributes the  
46 bulk of heating in *P. bipinnatifidum*. Fine scale regulation of AOX activity is post-  
47 translational. We also demonstrate that elevated O<sub>2</sub> can aid measurement of respiratory  
48 pathway fluxes in dense tissues.

## 50 **Key Words**

51 Alternative oxidase (AOX), Araceae, diffusion limitation, *Philodendron bipinnatifidum*, plant  
52 uncoupling proteins (pUCPs), plant thermogenesis, stable isotope measurements of respiration.

53 **Introduction**

54 Thermogenesis in the reproductive organs of plants is known to occur in the Cycadaceae (Tang *et al.*, 1987), and in Angiosperms, including both eudicots (e.g. Nelumbonaceae; Miyake, 1898) and  
55 *al.*, 1987), and in Angiosperms, including both eudicots (e.g. Nelumbonaceae; Miyake, 1898) and  
56 monocots (e.g. Araceae; Lance, 1974). The Araceae contains more thermogenic species than any  
57 other family (Meeuse, 1975; Meeuse & Raskin, 1988; Gibernau *et al.*, 2005), and has attracted  
58 much attention from researchers aiming to understand heating mechanisms (Wagner *et al.*, 1998;  
59 Ito *et al.*, 2003; Crichton *et al.*, 2005; Ito & Seymour, 2005; Onda *et al.*, 2008; Wagner *et al.*,  
60 2008), or to characterise the ecological significance of thermogenesis in plant-pollinator  
61 interactions (Gottsberger, 1999; Gibernau & Barabé, 2002). Amongst thermogenic arums, the  
62 capacity for heat generation differs markedly, from approximately 1-2°C above ambient  
63 temperature in *Monstera obliqua* (Chouteau *et al.*, 2007) to 34°C above in *Philodendron*  
64 *bipinnatifidum* (syn. *P. selloum*; Nagy *et al.*, 1972; Seymour *et al.*, 1983). In addition to this  
65 substantial thermogenic capacity, *P. bipinnatifidum* is also noteworthy as one of a small number  
66 of thermogenic species that can maintain a relatively constant floral temperature by regulating  
67 heat production in response to variations in ambient air temperature (Nagy *et al.*, 1972; Knutson,  
68 1974; Seymour & Schultze-Motel, 1996). Despite the attention they have received, the specific  
69 mechanisms of heating and thermoregulation have yet to be determined in the thermogenic  
70 Araceae, including *P. bipinnatifidum*.

71

72 Respiration using the ubiquitous cytochrome *c* oxidase (COX) pathway is coupled to ATP  
73 production. By contrast, in thermogenic plants, heat generation occurs via high respiratory fluxes  
74 uncoupled from ATP production, by two possible mechanisms. The first is the alternative  
75 pathway of respiration, which branches from the main mitochondrial electron transport chain at  
76 ubiquinone and for which the alternative oxidase (AOX) is the terminal oxidase. This pathway  
77 bypasses two sites of proton translocation (complexes III and IV), but can still be coupled to  
78 electron transport at a third site, complex I. Ubiquitous in plants (Vanlerberghe & McIntosh,

79 1997), and expressed at high levels in thermogenic tissues (Grant *et al.*, 2008), *AOX* genes are  
80 also present in fungi, protists and many animal lineages (McDonald & Vanlerberghe, 2006;  
81 McDonald, 2008). The second possible mechanism for heat generation involves plant uncoupling  
82 proteins (pUCPs) which act by dissipating the electrochemical gradient, and uncoupling  
83 respiratory electron transport from ATP regeneration. Whilst pUCPs are often assumed to only  
84 uncouple the COX pathway it is also possible that pUCPs could totally uncouple the AOX  
85 pathway to generate maximum heat. Some literature has suggested that substrates utilised can  
86 indicate the pathway responsible for heating (Sluse *et al.*, 1998; Ito & Seymour, 2005). Lipids,  
87 the major substrate for UCP1 mediated non-shivering thermogenesis in mammalian brown  
88 adipose tissue (Lowell & Spiegelman, 2000) are therefore assumed to also be the substrate for  
89 pUCPs. Conversely, it is often assumed that the AOX pathway utilises carbohydrate rather than  
90 lipid metabolism as free fatty acids have been found to inhibit AOX activity *in vitro* (Sluse *et al.*,  
91 1998).

92  
93 The only means to definitively demonstrate that AOX is involved in heat production *in vivo* is to  
94 quantify alternative pathway flux using stable O<sub>2</sub> isotope discrimination techniques (Ribas-Carbo  
95 *et al.*, 1995; Day *et al.*, 1996). Using this approach with thermoregulatory sacred lotus (*Nelumbo*  
96 *nucifera*), it has been demonstrated that up to 93% of total respiration was via the AOX pathway  
97 in heating flowers (Watling *et al.*, 2006; Grant *et al.*, 2008). Subsequent protein and substrate  
98 data demonstrated that AOX is solely responsible for heat generation in this eudicot (Grant *et al.*,  
99 2008; Grant *et al.*, in press). Measurements of respiratory fluxes and discrimination using isotope  
100 techniques have not been possible in thermogenic Araceae to date because of the high diffusional  
101 resistances in these structurally dense tissues (Guy *et al.*, 1989).

102  
103 The majority of studies of *P. bipinnatifidum* have focused on heating in the band of SM florets  
104 (Nagy *et al.*, 1972; Seymour *et al.*, 1984; Seymour, 1999) which are the source of up to 70% of

105 inflorescence heat (Seymour, 1999). Based largely on transcript abundances in different tissues, it  
106 has been suggested that pUCPs are the likely mechanism for thermogenesis in SM florets of *P.*  
107 *bipinnatifidum* (Ito & Seymour, 2005). Furthermore, a respiratory quotient of 0.83 has been  
108 reported for *P. bipinnatifidum* consistent with respiration switching from carbohydrate to lipid  
109 metabolism prior to heating (Walker *et al.*, 1983; Seymour *et al.*, 1984) and thus also implicating  
110 pUCPs. *AOX* transcripts however, also appeared to increase in heating SM florets of this species  
111 (Ito & Seymour, 2005). Importantly transcript abundance is not necessarily correlated with  
112 protein abundance or enzyme activity, and expression of *AOX* and pUCP in non-thermogenic  
113 and thermogenic tissues of *P. bipinnatifidum* has not been investigated. Co-expression of both  
114 pUCP and *AOX* proteins has been reported in thermogenic tissues of some other aroids,  
115 suggesting the possibility that both may play a role in thermogenesis (Onda *et al.*, 2008; Wagner  
116 *et al.*, 2008).

117

118 This study used *P. bipinnatifidum* as a model for the first *in vivo* measurements of *AOX* pathway  
119 flux during thermogenesis in an arum. Specifically we aimed to investigate whether isotopic  
120 discrimination was affected by diffusion during peak respiration in SM florets, by conducting  
121 measurements under different O<sub>2</sub> partial pressures. We also characterised heating patterns and  
122 mechanisms in the little studied fertile male (FM) florets. Here we present physiological and  
123 biochemical data that support a major role for *AOX* in heating in both SM and FM florets of *P.*  
124 *bipinnatifidum in vivo*. We also show how diffusional limitations to discrimination in dense  
125 tissues can be largely overcome by measuring stable O<sub>2</sub> isotope discrimination under elevated O<sub>2</sub>.

126

127 ***Materials and Methods***

128 *Plant Material*

129 *Philodendron bipinnatifidum* Schott ex Endl. (syn. *P. selloum* K.Koch.) spadices were sampled  
130 from the Adelaide Botanic Gardens, South Australia, and a private garden in Wollongong, New  
131 South Wales during November to December, 2006 and 2007. In Adelaide, spadices were sampled  
132 at five of the six developmental stages described below; we were not able to access plants to  
133 capture stage D. The entire spadix was removed and transported to the lab in a sealed plastic bag.  
134 Spadices were immediately dissected into floret types for respiration measurements, and protein  
135 and substrate analyses. Samples for mitochondrial protein analysis were stored on ice, and tissue  
136 samples for substrate analysis (lipid, carbohydrate) were snap frozen in liquid N<sub>2</sub> and stored at –  
137 80°C until analysed.

138

139 Further measurements of respiration and oxygen isotope discrimination were undertaken during  
140 the Northern summer, June-July 2009, using plants from private gardens in Palo Alto, California.

141

142 *Thermogenic stages*

143 Temperatures of SM and FM florets, non-thermogenic spathe tissue, and air were logged every  
144 three min, throughout the three to four day flowering period using ThermoChron i-Buttons  
145 (Maxim Integrated Products, Inc, Sunnyvale, CA). When inflorescences were sampled, air and  
146 floret temperatures, including non-thermogenic female florets and spathe temperature, were taken  
147 using a needle thermocouple inserted into the florets and a Fluke model 52 digital thermometer  
148 (Fluke Corp., Everett, WA, USA). There was no significant difference between i-Button and  
149 thermocouple temperatures. Nor were there significant differences between heating of  
150 inflorescences in Adelaide, Wollongong or Palo Alto.

151



152 Independence of heating in FM and SM florets was assessed by dissecting the spadix into three  
153 sections: female florets, FM florets and SM florets. Floret temperatures for each section, and non-  
154 thermogenic spathe temperature were logged in the laboratory (RT=approx. 24°C) using i-  
155 Buttons over two days.

156

157 Several distinct stages were identified, similar to those described in Seymour (1999) based on the  
158 heating pattern of the SM florets. The six stages were: pre-thermogenesis (stage A); shoulder  
159 (stage B), an initial phase of increasing temperature; peak thermogenesis (stage C), a distinct  
160 burst of heating of relatively short duration (< 1 h); the dip (stage D), a sharp decline in  
161 temperature after stage C; the plateau (stage E), 8-12 h of relatively constant elevated  
162 temperature; and post-thermogenesis (stage F), when heating has ceased after the pollen is shed  
163 toward the end of the plateau (Fig. 1).

164

#### 165 *Respiration and Discrimination Analysis*

166 Oxygen isotope discrimination during respiration of FM and SM florets, at each developmental  
167 stage, was determined using the on-line oxygen isotope technique described in Watling *et al.*  
168 (2006). The isotopic discrimination factors (D) and partitioning of electrons between the  
169 cytochrome and alternative pathways were calculated as previously described (Guy *et al.*, 1989;  
170 Henry *et al.*, 1999). The  $r^2$  of all unconstrained linear regressions between  $-\ln f$  and  $\ln (R/R_0)$ ,  
171 with a minimum of six data points, was at least 0.992. Discrimination endpoints for the  
172 alternative ( $\Delta a = 25.6 \pm 1.2\text{‰}$ ; mean  $\pm$  SD) and cytochrome ( $\Delta c = 16.4 \pm 2.9\text{‰}$ ) oxidases were  
173 determined (using SM and FM florets incubated with either 16 mM KCN or 25 mM SHAM (in  
174 0.05% DMSO), respectively) and used to calculate flux through the alternative and cytochrome  
175 pathways in uninhibited tissues as described in Ribas-Carbo *et al.*, (2005). Female florets are not

176 thermogenic, and preliminary measurements found very low respiration rates, hence no further  
 177 analyses were performed.

178

179 Because diffusional limitations in dense tissues can influence accurate determination of  $D$ , further  
 180 measurements were made under a range of  $O_2$  partial pressures. Biochemical discrimination  
 181 during respiration is a function of the ratio of internal to ambient  $O_2$  partial pressures ( $P_i/P_a$ ) as  
 182 described by equation 1 (Angert & Luz, 2001).

183

$$184 \quad D_{\text{total}} = D_d + (D_r - D_d)P_i/P_a \quad (1)$$

185

186 Where,  $D_{\text{total}}$  is the measured discrimination, which is a function of  $D_d$ , the discrimination due to  
 187 diffusion through the tissues (florets),  $D_r$ , biochemical discrimination occurring during  
 188 respiration, and  $P_i/P_a$  (i.e. diffusion from air into the tissues). Diffusion through floret tissue is  
 189 assumed to be in liquid phase, and thus discrimination will be negligible (Farquhar & Lloyd,  
 190 1993). Thus,  $D_d = 0$  in this case. Equation 1 then simplifies to:

191

$$192 \quad D_{\text{total}} = D_r * P_i/P_a \quad (2)$$

193

194 From Equation 2, it follows that if  $P_i/P_a$  is low, then accurate determination of discrimination  
 195 during respiration will not be possible. To determine whether oxygen isotope fractionation was  
 196 diffusionaly limited during peak heating, we made measurements on stage C, SM florets over a  
 197 range of  $O_2$  partial pressures, from ambient (21%  $O_2$ ) to three times ambient (63%  $O_2$ ) by  
 198 introducing pure  $O_2$  into the chamber. Mean endpoints for SM florets under elevated  $O_2$  were ( $\Delta a$   
 199 =  $27.1 \pm 1.0\text{‰}$  and  $\Delta c = 18.3 \pm 0.5\text{‰}$ ; mean  $\pm$  SD). Measurements in air immediately following  
 200 those made under increased  $O_2$  supply indicated that there was no oxygen toxicity with total

201 respiration rates unchanged by O<sub>2</sub> elevation (Supporting Information Fig. S1). These experiments  
202 were conducted in Palo Alto.

203

#### 204 *Isolation of Mitochondrial Proteins*

205 Isolation of washed mitochondrial proteins was based on the method of Day *et al.* (1985). The  
206 preparation of mitochondrial proteins, and protein quantification followed methods described in  
207 Grant *et al.* (2008). Protein concentrations were determined using the method of Bradford (1976)  
208 with known quantities of BSA as standards.

209

#### 210 *SDS-PAGE and immunoblotting*

211 Mitochondrial proteins separated by SDS-PAGE were transferred to PVDF membranes and  
212 detected by chemiluminescence as previously described (Grant *et al.*, 2008). Immunoblotting was  
213 performed using the mouse monoclonal primary antibodies AOA (1:500, raised against the  
214 alternative oxidase of *Sauromatum guttatum* Schott; Elthon *et al.*, 1989) and *PM035* from the  
215 mitochondrial marker protein porin (1:500, raised against *Zea mays* purified porin protein, Dr T  
216 Elthon, Lincoln, NE, USA). The rabbit polyclonal primary antibodies used were anti-COXII  
217 (1:1000, raised against subunit II of cytochrome *c* oxidase, Agrisera) and anti-SoyUCP (1:10 000,  
218 raised against *Glycine max* L. Merr purified pUCP; Considine *et al.*, 2001). For detection of  
219 AOX, pUCP and COXII, 60 µg of mitochondrial protein was loaded while only 10 µg was  
220 needed for detection of porin. AOX, pUCP and COXII protein levels are given relative to porin  
221 which acts as a loading control (Pring *et al.*, 2006). The total amount of mitochondrial protein  
222 extracted (g<sup>-1</sup> FW), and porin levels were similar across all developmental stages in all florets  
223 (data not shown). The AOX protein was present in the reduced and oxidised form; therefore  
224 mitochondrial isolates were incubated in the presence of 5mM DTT to completely reduce the  
225 protein. Serial dilutions confirmed linearity of the response of all proteins. Chemiluminescence

226 (SuperSignal West Femto Maximum Sensitivity Substrate; Pierce, Rockford, IL, USA) was used  
227 for the detection of the horse radish peroxidase-conjugated secondary antibodies. Densitometry  
228 quantification of the protein bands was made by a Fluorchem 8900 Gel Imager (Alpha Innotech,  
229 San Leandro, CA) with subsequent analysis using Fluorchem IS-8900 software (Alpha Innotech,  
230 San Leandro, CA).

231

### 232 *Soluble carbohydrate and starch determination*

233 *Philodendron bipinnatifidum* florets from each stage were assayed for soluble carbohydrates and  
234 starch as described in Grant *et al.* (2008). Briefly, soluble carbohydrates were extracted by  
235 heating florets (mean 0.023 g FW) in 80% ethanol (solvent:tissue, 30:1, v/w) at 70°C for 10 min.  
236 Glucose (glc), fructose (fru) and sucrose (suc) were determined sequentially following the  
237 addition of hexokinase (0.5U; Roche 1426362), phosphoglucose isomerase (0.6U; Roche  
238 127396) and invertase (8U; Sigma I-4504), respectively. Absorbance was measured at 340 nm  
239 using a SpectraMax Plus 384 microplate reader (Molecular Devices, Sunnyvale, CA). Starch was  
240 determined from the remaining tissue, which was ground in H<sub>2</sub>O, autoclaved, and incubated with  
241  $\alpha$ -amylase (20U; Sigma A-3176) and amyloglucosidase (14U; Fluka 10115) at 37°C for 4.5 h to  
242 convert starch to glc. An aliquot was then assayed for glc as described above.

243

### 244 *Lipid analysis*

245 Total lipid was extracted from 0.4 g of frozen floret tissue using standard methods (Folch *et al.*,  
246 1957) with minor changes as described. The frozen tissue was ground to a fine powder in liquid  
247 N<sub>2</sub> using a mortar and pestle and further homogenised with 10 ml of chloroform:methanol (2:1,  
248 v/v) containing butylated hydroxytoluene (0.01%, w/v) as an antioxidant. The homogenised  
249 samples were incubated at 4°C overnight on a rotator. Total lipids were separated into  
250 triacylglycerides (TAG - neutral lipids) and phospholipids (PL - charged lipids) by sequential

251 elution from Sep-Pac silica columns (Waters, Milford, MA) with hexane and ethyl acetate,  
252 respectively. Samples were dried at 37°C under N<sub>2</sub> in pre-weighed vials. Fatty acid composition  
253 of TAGs was then determined. Samples were trans-methylated using the method of Lepage and  
254 Roy (1986). The fatty acid methyl esters were separated by gas-liquid chromatography on a  
255 Shimadzu GC 17A (Shimadzu, Sydney, Australia) with a Varian WCOT Fused Silica Column  
256 (50 m x 0.25 mm ID, CP7419, Sydney, Australia). Fatty acids were identified using retention  
257 times of an external standard (F.A.M.E Supelco, Bellefonte, PA), and quantified against a  
258 heneicosanoic acid (21:0) internal standard (Sigma Aldrich, Sydney, Australia).

259

## 260 *Statistical Analysis*

261 Changes in respiratory pathways and relative AOX, COXII and pUCP protein with respect to  
262 developmental stage and between floret types were investigated by analysis of variance  
263 (ANOVA). Where ANOVA revealed significant differences, Tukey HSD post hoc tests were  
264 applied in order to identify significantly different means. Data were tested for normality using the  
265 Shapiro-Wilk W Test. Bartlett's test was applied to ensure homogeneity of variances. Where  
266 these assumptions were not satisfied, data were square root or cube root transformed before  
267 analysis. All analyses were undertaken using JMP 5.1 (SAS Institute Inc.).

268

## 269 *Results*

### 270 *Characterisation of thermogenesis*

271 The pattern of heating for SM florets was similar to that reported by Seymour (1999), but we also  
272 observed a distinct and independent pattern of heating in the FM florets, that has not previously  
273 been reported in *P. bipinnatifidum*. Mean FM floret temperature at peak thermogenesis (stage C)  
274 was 5.5°C lower than in SM florets ( $t_{26,0}=8.2$ ,  $P<0.0001$ ; Table I), but there were no significant

275 differences in mean temperatures between floret types at other thermogenic stages (Table I). At  
 276 peak thermogenesis mean FM floret temperature ranged from 34.0 to 38.1°C ( $35.7 \pm 1.4^\circ\text{C}$ , mean  
 277  $\pm$  SD,  $n=14$ ) against ambient temperatures ranging from 15 to 30.2°C. Peak temperatures in SM  
 278 florets ranged from 37 to 41.5°C ( $40.1 \pm 1.4^\circ\text{C}$ ,  $n=14$ ) across the same range of air temperatures.  
 279 The slope of the linear regression between peak (stage C) temperature and ambient temperature  
 280 ( $T_a$ ) in FM florets (FM peak  $T = 0.18 * T_a + 31.1$ ;  $P=0.04$ ) was significantly different from unity  
 281 ( $t_{14}=6.7$ ,  $P<0.05$ ), but similar to zero indicating strong thermoregulation. SM florets also  
 282 regulated peak temperature; the slope of the SM floret peak temperature versus  $T_a$  relationship  
 283 was 0.14, similar to previously reported values for SM florets (Nagy *et al.*, 1972; Seymour *et al.*,  
 284 1983). Peak temperatures of FM and SM florets were not correlated with either total spadix mass,  
 285 or the mass of the specific floret types (data not shown). Dip (stage D) temperatures remained  
 286 above ambient in both SM and FM florets (Table I). FM florets reached their minimum  
 287 temperature earlier than SM florets, and began to increase earlier to the thermoregulatory plateau  
 288 (stage E), during which they maintained a mean temperature of  $29.0 \pm 1.6^\circ\text{C}$  for 8 to 12 h by  
 289 heating from 2 to 11.1°C above ambient temperature (Fig 1). The period of temperature  
 290 regulation at stage E was of longer duration in FM florets than SM florets, which maintained a  
 291 similar mean plateau temperature ( $28.8 \pm 2.2^\circ\text{C}$ ; Table I).

292

293 SM and FM florets from dissected spadices continued to heat *ex planta* and exhibited the same  
 294 pattern of heating as intact inflorescences, for up to 30 h after detachment (Fig. 1b,c). When  
 295 detached late during stage B (5 pm) peak thermogenesis was achieved rapidly, FM and SM  
 296 florets reaching maxima of 37.7°C and 39.8°C, respectively (Fig. 1b). If florets were sampled  
 297 earlier during stage B (1 pm), the peak was broader, and maxima lower (33.3°C and 36.7°C for  
 298 FM and SM florets, respectively; Fig. 1c). All maxima were within the range of peak  
 299 temperatures recorded for intact spadices (Table I).

300

301 *Respiratory fluxes*

302 Mean total respiratory flux increased 2.6-fold with the onset of heating in FM florets ( $F_{3,21}=4.2$ ,  
303  $P=0.0200$ ; Fig. 2a). This increase was largely accounted for by the significant 3.8-fold increase in  
304 AOX flux from  $0.013 \pm 0.006 \mu\text{mol O}_2 \text{ g FW}^{-1} \text{ s}^{-1}$  in stage A (pre-thermogenesis) to its maximum  
305 mean value of  $0.051 \pm 0.013 \mu\text{mol O}_2 \text{ g FW}^{-1} \text{ s}^{-1}$  at stage B ( $F_{3,21}=3.4$ ,  $P=0.0421$ ; Fig. 2a). Across  
306 the thermogenic stages (B-E), AOX accounted for, on average, between 44.2 and 74.2% of total  
307 respiratory flux in FM florets, and the highest proportion of flux via AOX was 92%. Mean COX  
308 flux comprised less than 41% of total flux in FM florets across thermogenic stages B-E, and was  
309 similar across all developmental stages (Fig. 2a). In FM florets, both discrimination (D;  $r^2=0.35$ ,  
310  $P=0.0029$ ) and AOX flux ( $r^2=0.77$ ,  $P<0.0001$ ) were strongly positively correlated with total  
311 respiratory flux (data not shown). That high AOX fluxes were measured when total respiration  
312 rates were high, suggests that oxygen fractionation in the FM floret tissue was not diffusionally  
313 limited, or that any limitation was minimal.

314

315 As stage C is brief, it is possible that inflorescences were sampled after peak temperature had  
316 been reached and it appears that peak fluxes in FM florets were not captured (cf. Fig. 2a & 2b),  
317 thus relationships between fluxes and heating in these florets were analysed excluding stage C  
318 samples. Total respiratory flux ( $\text{flux}=0.0074*\text{heating}+0.016$ ,  $r^2=0.55$ ,  $P=0.0007$ ; Fig. 3a) and  
319 AOX flux ( $\text{flux}=0.0062*\text{heating}+0.0022$ ,  $r^2=0.60$ ,  $P=0.0003$ ; Fig. 3c), were significantly  
320 positively correlated with heating in FM florets, variation in AOX flux accounting for 60% of the  
321 variation in floret heating across all thermogenic stages. Consistent with the absence of  
322 substantial changes in COX flux between developmental stages (Fig. 2a), there was no  
323 correlation between COX flux and heating in FM florets (Fig. 3c).

324

325 Respiratory fluxes in SM florets differed from those in FM florets across the developmental  
326 stages (Fig. 2b). Mean total respiratory flux increased significantly with the onset of

327 thermogenesis ( $F_{3,20}=8.40$ ,  $P=0.0012$ ), and continued to increase to peak thermogenic stage C  
328 when the highest respiratory flux in either floret was recorded ( $0.106 \pm 0.013 \mu\text{mol O}_2 \text{ g FW}^{-1} \text{ s}^{-1}$ ;  
329 Fig. 2b). This suggests that peak fluxes associated with maximum heating in SM florets at stage  
330 C were captured (Fig. 2b); thus they were included in regression analysis (Fig. 3b). As in FM  
331 florets, there was a significant positive correlation between total respiratory flux and heating in  
332 SM florets ( $\text{flux}=0.0060*\text{heating}+0.0090$ ,  $r^2=0.78$ ,  $P<0.0001$ ; Fig. 3b). In contrast, however,  
333 apparent AOX flux in SM florets remained low throughout development (Fig. 3d) and was less  
334 than one third of the maximum AOX flux recorded in FM florets ( $0.094 \mu\text{mol O}_2 \text{ g FW}^{-1} \text{ s}^{-1}$ ; Fig.  
335 3c).

336  
337 To investigate whether these apparently low AOX fluxes were a consequence of diffusion  
338 influencing discrimination between isotopes (Ribas-Carbo *et al.*, 2005) we made measurements  
339 during peak heating under a range of  $\text{O}_2$  partial pressures. Diffusional limitation to fractionation  
340 could occur in dense tissues because of the greater depletion of  $^{16}\text{O}$  relative to  $^{18}\text{O}$ , leading to a  
341 change in the intracellular isotope ratio of the source gas (Guy *et al.*, 1989). These  $\text{O}_2$   
342 experiments demonstrated a clear diffusional effect on isotopic discrimination in strongly heating  
343 tissues, as total respiratory flux did not increase with increased  $\text{O}_2$  supply, however, D values did  
344 (Fig. 4 and Table II). In contrast to measurements made in air, where mean AOX fluxes were  
345 only  $15.7 \pm 4.5\%$ , the mean AOX flux in stage C SM florets was  $70.8 \pm 2.5\%$  under increased  $\text{O}_2$   
346 (Table II). We found no evidence of any toxic effects of elevated  $\text{O}_2$  on these tissues (Fig. 4;  
347 Supporting Information Fig. S1), nor was there any evidence that AOX activity was stimulated  
348 by elevated  $\text{O}_2$  as: (1) total respiration did not change with  $\text{O}_2$  in either floret type (Fig. 4 for SM  
349 florets), (2) in SM florets with lower respiration rates, consecutive measures in air and  $\text{O}_2$   
350 provided identical low values for both AOX and total respiratory flux, and (3) similarly high  
351 AOX fluxes were recorded in both air and elevated  $\text{O}_2$  in FM tissues (data not shown). Thus the  
352 use of elevated  $\text{O}_2$  did not alter the AOX flux, rather it altered our ability to measure AOX flux



353 accurately, especially in the strongly respiring (heating) stage C florets (Table II; Supporting  
354 Information Fig. S1).

355

356 As respiration was saturated at 21% O<sub>2</sub> (Fig. 4), increasing O<sub>2</sub> partial pressures will result in an  
357 increase in Pi/Pa, thus largely overcoming the diffusional limitation observed at 21% O<sub>2</sub> and  
358 enabling more accurate measurement of true discrimination. This is illustrated by the theoretical  
359 response of Dt to changes in O<sub>2</sub> concentration, determined using equation 2. In this example,  
360 Dr=27.1 (the discrimination endpoint for AOX measured under elevated O<sub>2</sub>), and Pi/Pa was  
361 determined using Equation 3 across Pa from 0 to 100%.

362

$$363 \quad P_i/P_a = (P_a - G)/P_a \quad (3)$$

364

365 Where G, the diffusion gradient (Pa-Pi), is a function of the diffusion resistance of the floret  
366 tissue (R), and the respiration rate (J), such that G=R\*J. We cannot measure R directly, but it was  
367 assumed to remain constant, and as there was no change in J as O<sub>2</sub>% increased above 21%, G  
368 should not change with O<sub>2</sub> (Fig. 4). Therefore, G was adjusted to fit the observed discrimination  
369 data, G=7.5% giving the best fit (Fig. 4). While this curve indicates that at Pa above 60% O<sub>2</sub> there  
370 will still be some diffusional limitation, it is clear that the error in measuring D at these O<sub>2</sub>  
371 concentrations (where Pi/Pa is at least 0.8) is very small, especially relative to biological  
372 variation. In addition, this approach provides the possibility of estimating R if Dr is known, and  
373 assumed not to change with O<sub>2</sub>.

374

### 375 *AOX, pUCP, and COXII proteins during thermogenesis*

376 In FM florets, there was a significant 5.4-fold increase in AOX protein (relative to porin) between  
377 stages A and B, corresponding with the onset of thermogenesis (Fig. 5a). Subsequently, AOX

378 levels remained high during the thermogenic stages B-E, and on average decreased by 62% post-  
379 thermogenesis between stages E and F, although this was not statistically significant (Fig. 5a).  
380 Similarly, the expression of COXII increased significantly (5.1-fold) between stages A and B  
381 with the onset of thermogenesis (Fig. 5d). COXII was then maintained at similar levels  
382 throughout subsequent developmental stages (Fig. 5d). By contrast, no significant increase in  
383 expression of pUCP was detected in FM florets either at the onset of thermogenesis (Fig. 5g), or  
384 in subsequent stages. There were no correlations between AOX, COXII or pUCP expression and  
385 heating in FM florets (data not shown), nor was there a correlation between AOX content and  
386 respiratory flux via the AOX in FM florets (data not shown). This was because levels of these  
387 proteins remained constant during stages B-E, while heating varied with changes in ambient  
388 temperature. Similarly, neither COXII nor pUCP content correlated with COX flux in FM florets  
389 (data not shown).

390

391 In SM florets, there was a trend towards increasing AOX with the onset of thermogenesis, and  
392 AOX then declined significantly between peak (stage C) and post-thermogenesis (stage F; Fig.  
393 5b). Similarly, there was a significant increase in expression of COXII from pre-thermogenesis to  
394 peak (stage C) followed by a significant decline (Fig. 5e). Despite a similar pattern of expression  
395 for pUCP, results for this protein were not significant (Fig. 5h). As with FM florets, there were no  
396 correlations between AOX, COXII or pUCP expression and heating in SM florets. Similarly,  
397 neither pUCP nor COXII protein expressions were correlated with respiratory flux via COX, nor  
398 were AOX content and AOX flux correlated (data not shown).

399

400 Mitochondrial proteins, AOX, COXII and pUCP (relative to porin), were similar across all stages  
401 in female florets (Fig. 5c,f,i). Relative AOX content was significantly lower in female florets  
402 (non-thermogenic) than SM and FM florets (2-way ANOVA,  $F_{2,7}=9.9$ ,  $P=0.002$ ; Fig. 5c). By  
403 contrast, relative COXII and pUCP contents were similar across all floret types (Fig. 5).

404

405 *Substrates - carbohydrates and lipids.*

406 Total triacylglyceride (TAG) concentrations were significantly higher in SM florets than FM

407 florets ( $F_{1,54}=23.4$ ,  $P<0.0001$ ; Fig. 6a,b) particularly across stages A-C. In SM florets, TAG

408 content decreased significantly, by 63%, from peak thermogenesis (stage C) to plateau (stage E;

409  $P<0.0001$ ; Fig. 6b). By contrast, in FM florets TAGs remained similar throughout pre-

410 thermogenic and thermogenic stages (A-E), only declining significantly post-thermogenesis once

411 pollen was shed ( $P=0.0031$ ; Fig. 6a). Total TAG content in both floret types was not significantly

412 correlated with either floret heating or respiratory fluxes across the developmental series (data not

413 shown).

414

415 Conversely, SM florets had significantly lower concentrations of starch than FM florets (2-way

416 ANOVA  $F_{1,53}=27.9$ ,  $P<0.0001$ ; Fig. 6c,d). Across stages A-E, mean starch concentrations of FM417 florets (mean  $\pm$  SE,  $5.0 \pm 0.6$  mg  $g^{-1}$  FW) were almost three times greater than SM florets ( $1.7 \pm$ 418  $0.3$  mg  $g^{-1}$  FW; Fig. 6c,d). Starch content was high in pre-thermogenic FM florets, and remained

419 similar throughout the thermogenic stages, declining significantly by 82% post-thermogenesis

420 (stage F; Fig. 6c). In contrast to FM florets, no significant change in starch content was detected

421 in SM florets across the developmental series (Fig. 6d). Starch content was not significantly

422 correlated with either floret heating or respiratory fluxes across the developmental series (data not

423 shown). Total soluble carbohydrate content of SM and FM florets was similar and did not vary

424 across stages (data not shown).

425

426 ***Discussion***

427 This study has three key findings. First, despite apparently using different fuels, heat production

428 in both fertile and sterile male florets of *P. bipinnatifidum* occurs predominantly via the

429 alternative pathway. Second, both male floret types can maintain their thermoregulatory activity  
430 *ex planta* for up to 30 h. Finally, with the exception of the sacred lotus (Watling *et al.*, 2006;  
431 Grant *et al.*, 2008), measurements of respiratory fluxes and discrimination using isotope  
432 techniques have not been possible in other thermogenic tissues to date because of the high  
433 diffusional resistances (Guy *et al.*, 1989). Our third key finding that diffusional effects on O<sub>2</sub>  
434 isotope discrimination in dense tissues can be largely overcome by using elevated O<sub>2</sub> partial  
435 pressures provides an important advance in stable isotope measurements of respiration.

436

#### 437 *Thermogenesis and thermoregulation by fertile male florets*

438 We demonstrated that fertile male (FM) florets heat in a pattern similar to that characterised for  
439 sterile male (SM) florets except that FM florets typically commenced heating earlier than SM  
440 florets, and had a less pronounced peak and dip than SM florets. Furthermore, measurements of  
441 dissected inflorescences in the lab demonstrated that both floret types heat independently.

442

443 In the current study, heating in both SM and FM florets lasted for at least 30 h following excision  
444 from the plant, and was similar to that recorded on intact inflorescences. This contrasts with  
445 previous studies reporting that excision of spadices from *P. bipinnatifidum* stimulates a  
446 respiratory burst lasting only 1-2 h, with respiration dropping to very low rates 2 h after removal  
447 from the plant (Seymour *et al.*, 1983; Seymour, 1991), but is similar to *P. melinonii* where  
448 isolated FM and SM florets heated for at least 14 h once cut from the plant (Seymour &  
449 Gibernau, 2008). The duration and magnitude of heating in isolated FM and SM florets suggests  
450 that all that is required for heat generation (e.g. fuel) and for temperature regulation (e.g.  
451 signalling) is contained within the detached inflorescence. Consistent with this, our data indicated  
452 that thermogenesis is unlikely to be limited by substrate (lipid or carbohydrate) supply.  
453 Calorimetric studies of *P. bipinnatifidum* spadices also concluded that there was no substrate

454 import into the inflorescence during thermogenesis (Seymour, 1991). In contrast, thermogenesis  
455 in other aroids, e.g. *Symplocarpus foetidus* (skunk cabbage) relies on carbohydrate import, and  
456 inflorescence heating ceases upon removal from the plant (Knutson, 1974; Ito, *et al.*, 2003).

457

#### 458 *Mechanisms of heating in P. bipinnatifidum*

459 We identified a clear relationship between *in vivo* alternative pathway (AOX) flux and heating in  
460 both FM and SM florets of *P. bipinnatifidum*. Based on our oxygen isotope measurements, the  
461 AOX pathway accounts for the bulk of respiratory activity in both of these thermogenic tissues,  
462 and indeed the proportions of flux via AOX in SM florets (96%) are the highest measured to date  
463 (Ribas-Carbo *et al.*, 2005; Watling *et al.*, 2006; Grant *et al.*, 2008). The high proportions of AOX  
464 flux in both FM (up to 92%) and SM florets are similar to those reported in the thermoregulatory  
465 receptacles of *N. nucifera* where up to 93% of respiration was via AOX in the most strongly  
466 heating flowers, and where AOX flux was strongly correlated with heating (Watling *et al.*, 2006;  
467 Grant *et al.*, 2008). Similarly, 78% of total respiratory flux was via the AOX in isolated  
468 mitochondria of thermogenic *Symplocarpus foetidus* (Guy *et al.*, 1989). In our study, SM florets,  
469 which reach the highest peak temperatures (Table I), also had the highest mean total respiration  
470 rate ( $0.15 \mu\text{mol O}_2 \text{ g FW}^{-1} \text{ s}^{-1}$ ; stage C), although peak respiration rates may not have been  
471 captured in FM florets (Fig 2a). Given the high proportional engagement of the alternative  
472 pathway in *P. bipinnatifidum* thermogenic tissues, fluxes via the AOX are substantial, up to  $0.094$   
473  $\mu\text{mol O}_2 \text{ g FW}^{-1} \text{ s}^{-1}$  and  $0.15 \mu\text{mol O}_2 \text{ g FW}^{-1} \text{ s}^{-1}$  in FM and SM florets, respectively.

474

475 Our finding that discrimination was essentially the same in FM florets in air or elevated  $\text{O}_2$   
476 suggests that diffusional limitations were not an issue with FM florets. In contrast, diffusional  
477 limitations to discrimination were observed in SM florets but were essentially overcome by  
478 increasing the  $\text{O}_2$  concentration, which confirmed that the majority of the respiratory flux in stage

479 C and E florets is via the AOX pathway. The use of higher O<sub>2</sub> partial pressures to largely mitigate  
480 the effects of diffusional limitations to discrimination in these dense tissues opens up the  
481 possibility of using stable isotope methodologies not only to measure alternative pathway flux in  
482 thermogenic plants, but also in other diffusionally limited tissues. That SM florets displayed O<sub>2</sub>  
483 diffusional limitations, but FM florets did not could be a result of the higher total respiration rates  
484 in SM florets, and/or be due to differences in floret morphology. For example, FM florets have a  
485 higher surface area to volume ratio and thinner cuticle than SM florets (Grant, 2010).

486

487 The strong relationship between AOX flux and heating in FM florets, and the substantial  
488 proportions of total flux via AOX in both FM and SM florets, suggest there is little room for  
489 contribution by pUCPs, except alongside AOX to totally uncouple respiration via concurrent  
490 operation of pUCPs and AOX (Onda *et al.*, 2008; Wagner *et al.*, 2008). If pUCPs alone were  
491 responsible for heat generation in *P. bipinnatifidum*, then we would expect an increase in flux  
492 through the cytochrome pathway during thermogenesis; however we detected no change in COX  
493 flux during heating by FM florets across all thermogenic stages, and comparatively low  
494 proportions of total flux via COX in peak heating SM florets when measured under increased O<sub>2</sub>  
495 supply. Our protein data further support the substantial role for AOX in thermogenesis in *P.*  
496 *bipinnatifidum*; whereas AOX increases in thermogenic tissues and stages, pUCP does not.  
497 Synchronicity between onset of thermogenic activity and the increase in AOX protein in both  
498 floret types is similar to the pattern found in sacred lotus (Grant *et al.*, 2008), but contrasts with  
499 other Araceae (e.g. *Sauromatum guttatum* and *Arum maculatum*) where significant increases in  
500 AOX protein precede the onset of thermogenesis by several days (Rhoads & McIntosh, 1992;  
501 Chivasa *et al.*, 1999).

502

503 Our data provide evidence for developmental regulation of thermogenesis at the level of protein  
504 synthesis in *P. bipinnatifidum*; however no significant relationship between AOX protein content  
505 and AOX flux was detected during the thermogenic stages. This indicates that fine scale post-  
506 translational regulation of AOX activity most likely occurs and is responsible for regulating heat  
507 production. Activation of AOX is controlled, in part, by the redox status of the protein which is  
508 regulated via the formation of disulfide bonds between conserved cysteine residues (Rhoads *et*  
509 *al.*, 1998). At least one isoform of AOX from *P. bipinnatifidum* contains the regulatory cysteines  
510 (Ito & Seymour, 2005; Grant *et al.*, 2009); however, around 40% of the protein resists oxidation  
511 by diamide (Grant, 2010) suggesting it may lack this redox control. The activity of the reduced  
512 protein can be further moderated by effectors such as  $\alpha$ -keto acids (e.g. pyruvate, succinate)  
513 (Rhoads *et al.*, 1998), the specific effector varying depending on the AOX isoform. For example,  
514 AOX from thermogenic *N. nucifera* also shows significant redox insensitivity, and stimulation of  
515 AOX occurs via succinate rather than pyruvate (Grant *et al.*, 2009). An AOX which is not redox  
516 regulated (Onda *et al.*, 2007; Grant *et al.*, 2009) but is controlled by effectors could provide  
517 greater control of AOX flux for the precise temperature control these plants achieve over a  
518 prolonged period. By contrast, AOX from *Sauromatum guttatum*, which does not thermoregulate  
519 but rather heats in a single burst (Meeuse, 1966; Meeuse & Raskin, 1988), is constitutively active  
520 (Crichton *et al.*, 2005).

521

522 The co-occurrence of AOX and pUCP in thermogenic tissues, such as *P. bipinnatifidum*, has  
523 raised speculation that both may contribute to heating, but to date there is little evidence that  
524 pUCPs function in heat generation in plants (Grant *et al.*, 2008; Wagner *et al.*, 2008). Based on  
525 *pUCP* and *AOX* transcript abundances, the mechanism of thermogenesis in *P. bipinnatifidum* was  
526 assumed to be pUCPs (Ito & Seymour, 2005); however, our data clearly demonstrate a  
527 predominant role for AOX in heating in this species. Between 70-96% of total flux was via the

528 alternative pathway in heating FM and SM florets, AOX protein increased specifically in  
529 thermogenic male tissues, and no significant difference in amounts of pUCP was found between  
530 non-thermogenic and thermogenic stages. If pUCP operated alongside AOX in these tissues we  
531 would expect concurrent increases in both proteins throughout thermogenesis. Intriguingly, we  
532 did observe an increase in COXII protein with the onset of thermogenesis in both FM and SM  
533 florets. Relative amounts, however, were very similar to those observed in non-thermogenic  
534 female florets unlike AOX protein which was several fold higher in male as compared to female  
535 florets.

536

537 Studies indicating that lipids were used as respiratory substrates in thermogenic *P. bipinnatifidum*  
538 florets have been used to support a role for pUCPs in thermogenesis in this species (Ito &  
539 Seymour, 2005). The assumption derives from the fact that lipids are the substrate for animal  
540 UCPs (Argyropoulos & Harper, 2002), and that fatty acids (e.g. linoleic acid) which stimulate  
541 pUCP inhibit AOX activity (Sluse *et al.*, 1998). Calorimetric studies yielding a respiratory  
542 quotient of 0.83, and C isotope analyses suggest that spadices switch from carbohydrate to direct  
543 lipid oxidation once the spathe opens and thermogenesis commences (Nagy *et al.*, 1972; Walker  
544 *et al.*, 1983; Seymour *et al.*, 1984). We found significant declines in lipid content (total TAGs)  
545 towards the end of the thermogenic phase and post-thermogenesis in both SM and FM florets,  
546 consistent with lipid oxidation during thermogenesis. In addition, in FM florets, concurrent with  
547 the decline in TAGs post-thermogenesis, total starch content also decreased significantly. It is  
548 difficult to draw definitive conclusions about the specific substrate for thermogenesis in FM  
549 florets because changes in starch and lipids during anthesis may also be associated with  
550 maturation of male florets. Nevertheless, the significant decline in starch in FM florets is similar  
551 to that recorded in other thermogenic species, including the sacred lotus receptacle (Grant *et al.*,  
552 2008), *Symplocarpus foetidus* and *Arum maculatum* (ap Rees *et al.*, 1976; ap Rees *et al.*, 1977).  
553 By contrast, other Araceae may use both lipids and carbohydrates (e.g. *Sauromatum guttatum*;



554 Wilson & Smith, 1971). Our flux and protein data strongly support a role for AOX and  
555 demonstrate that AOX and pUCP activity can not be inferred based on substrate type alone. It  
556 does seem, however, that lipids are the major substrate for thermogenesis in SM florets of *P.*  
557 *bipinnatifidum*. If so, this suggests that AOX activity may not be as sensitive to fatty acids in  
558 these tissues as has been observed in non-thermogenic plants such as tomato (Sluse *et al.*, 1998).  
559

### 560 *Conclusion*

561 In summary, we have shown that both sterile and fertile male florets of *P. bipinnatifidum* have  
562 independent thermoregulatory phases that persist *ex planta*. Thermogenic activity is driven  
563 predominantly via increased flux through the alternative respiratory pathway in both floret types.  
564 Whilst increased expression of AOX protein during the thermogenic phase provides the capacity  
565 for the increased AOX flux, fine scale regulation of AOX activity must also occur. Although both  
566 floret types primarily use the alternative pathway to produce heat, the respiratory fuel appears to  
567 differ with lipids and carbohydrates more predominant in SM and FM florets, respectively. A  
568 further important finding of this study is that diffusional limitations, that have to date prevented  
569 measurements of oxygen fractionation in most thermogenic species, can be mostly overcome, or  
570 potentially estimated, as a result of measurement at elevated partial pressures of oxygen. This  
571 latter finding provides an important advance to studies aimed at understanding the mechanisms  
572 that regulate heating in thermogenic plants, and roles of AOX in dense tissues of non-  
573 thermogenic plants. This study clearly demonstrates the importance of functional measurements  
574 of respiratory pathways to compliment molecular studies.

575

### 576 *Acknowledgments*

577 Thanks are due to the Adelaide and Wollongong Botanic Gardens, Marisa Collins, Ben Licht,  
578 Steve Smith and Terry Shuchat for access to *P. bipinnatifidum* plants. Antibodies were kindly

579 donated by Murray Badger (Australian National University, Australia), James Whelan  
580 (University of Western Australia, Australia) and Kikukatsu Ito (Iwate University, Japan). Thanks  
581 also to Beth Guy for assistance with measurements in California. This work was supported by the  
582 Australian Research Council (grant no. DP0451617) and The Hermon Slade Foundation  
583 (HSF09/7). NMG received an Australian Postgraduate Award Studentship.

## References

- Angert A, Luz B. 2001.** Fractionation of oxygen isotopes by root respiration: Implications for the isotopic composition of atmospheric O<sub>2</sub>. *Geochimica et Cosmochimica Acta* **65**(11): 1695-1701.
- ap Rees T, Fuller WA, Wright BW. 1976.** Pathways of carbohydrate oxidation during thermogenesis by the spadix of *Arum maculatum*. *Biochimica et Biophysica Acta* **437**: 22-35.
- ap Rees T, Wright BW, Fuller WA. 1977.** Measurements of starch breakdown as estimates of glycolysis during thermogenesis by the spadix of *Arum maculatum* L. *Planta* **134**: 53-56.
- Argyropoulos G, Harper M-E. 2002.** Molecular biology of thermoregulation: Invited review: Uncoupling proteins and thermoregulation. *Journal of Applied Physiology* **92**(5): 2187-2198.
- Chivasa S, Berry JO, ap Rees T, Carr JP. 1999.** Changes in gene expression during development and thermogenesis in *Arum*. *Australian Journal of Plant Physiology* **26**: 391-399.
- Bradford MM. 1976.** A rapid and sensitive method for the quantitation of microgram quantities of protein utilizing the principle of protein-dye binding. *Analytical Biochemistry* **72**: 248-254.
- Chouteau M, McClure M, Gibernau M. 2007.** Pollination ecology of *Monstera obliqua* (Araceae) in French Guiana. *Journal of Tropical Ecology* **23**(05): 607-610.
- Considine MJ, Daley DO, Whelan J. 2001.** The expression of alternate oxidase and uncoupling protein during fruit ripening in mango. *Plant Physiology* **126**: 1619-1629.
- Crichton PG, Affourtit C, Albury MS, Carre JE, Moore AL. 2005.** Constitutive activity of *Sauromatum guttatum* alternative oxidase in *Schizosaccharomyces pombe* implicates residues in addition to conserved cysteines in  $\alpha$ -keto acid activation. *FEBS Letters* **579**(2): 331-336.
- Day DA, Krab K, Lambers H, Moore AL, Siedow JN, Wagner AM, Wiskich JT. 1996.** The cyanide-resistant oxidase: To inhibit or not to inhibit, that is the question. *Plant Physiology* **110**: 1-2.
- Day DA, Neuburger M, Douce R. 1985.** Biochemical characterization of chlorophyll-free mitochondria from pea leaves. *Australian Journal of Plant Physiology* **12**: 219-228.
- Elthon TE, Nickels RL, McIntosh L. 1989.** Monoclonal antibodies to the alternative oxidase of higher plant mitochondria. *Plant Physiology* **89**(4): 1311-1317.
- Farquhar GD, Lloyd J 1993.** Carbon and oxygen isotope effects in the exchange of carbon dioxide between terrestrial plants and the atmosphere. In: J. R. Ehleringer, A. E. Hall, G. D. Farquhar eds. *Stable isotopes and plant carbon-water relations*. San Diego: Academic Press, 47-70.
- Folch J, Lees M, Sloane-Stanley G. 1957.** A simple method for the isolation and purification of total lipids from animal tissue. *Journal of Biological Chemistry* **226**: 497-509.
- Gibernau M, Barabé D. 2002.** Pollination ecology of *Philodendron squamiferum* (Araceae). *Canadian Journal of Botany* **80**(3): 316-320.
- Gibernau M, Barabé D, Moisson M, Trombe A. 2005.** Physical constraints on temperature difference in some thermogenic aroid inflorescences. *Annals of Botany* **96**: 117-125.
- Gottsberger G. 1999.** Pollination and evolution in neotropical Annonaceae. *Plant Species Biology* **14**(2): 143-152.
- Grant N, Onda Y, Kakizaki Y, Ito K, Watling J, Robinson S. 2009.** Two cys or not two cys? That is the question; alternative oxidase in the thermogenic plant sacred lotus. *Plant Physiology* **150**(2): 987-995.

- Grant NM. 2010.** *Thermogenesis in plants: The mode of heating and regulation in hot flowers.* PhD thesis, University of Wollongong Wollongong, NSW, Australia.
- Grant NM, Miller RE, Watling JR, Robinson SA. 2008.** Synchronicity of the thermogenic activity, alternative pathway respiratory flux, AOX protein content, and carbohydrates in receptacle tissues of sacred lotus during floral development. *Journal of Experimental Botany* **59**(3): 705-714.
- Grant NM, Miller RE, Watling JR, Robinson SA. in press.** Distribution of thermogenic activity in floral tissues of *Nelumbo nucifera*. *Functional Plant Biology*, in press.
- Guy R, Berry JA, Fogel ML, Hoering TC. 1989.** Differential fractionation of oxygen isotopes by cyanide-resistant and cyanide-sensitive respiration in plants. *Planta* **177**: 483-491.
- Henry B, Atkin OK, Day DA, Millar AH, Menz RI, Farquhar G. 1999.** Calculation of the oxygen isotope discrimination factor for studying plant respiration. *Australian Journal of Plant Physiology* **26**: 773-780.
- Ito K, Abe Y, Johnston SD, Seymour RS. 2003.** Ubiquitous expression of a gene encoding for uncoupling protein isolated from the thermogenic inflorescence of the dead horse arum *Helicodiceros muscivorus*. *Journal of Experimental Botany* **54**(384): 1113-1114.
- Ito K, Onda Y, Sato T, Abe Y, Uemura M. 2003.** Structural requirements for the perception of ambient temperature signals in homeothermic heat production of skunk cabbage (*Symplocarpus foetidus*). *Plant, Cell and Environment* **26**: 783-788.
- Ito K, Seymour R. 2005.** Expression of uncoupling protein and alternative oxidase depends on lipid or carbohydrate substrates in thermogenic plants. *Biological Letters* **1**(4): 427-430.
- Knutson RM. 1974.** Heat production and temperature regulation in eastern skunk cabbage. *Science* **186**: 746-747.
- Lance PC. 1974.** Respiratory control and oxidative phosphorylation in *Arum maculatum* mitochondria. *Plant Science Letters* **2**: 165-171.
- Lepage G, Roy CC. 1986.** Direct transesterification of all classes of lipids in a one-step reaction. *Journal of Lipid Research* **27**(1): 114-120.
- Lowell BB, Spiegelman BM. 2000.** Towards a molecular understanding of adaptive thermogenesis. *Nature* **404**(6778): 652-660.
- McDonald AE. 2008.** Alternative oxidase: An inter-kingdom perspective on the function and regulation of this broadly distributed 'cyanide-resistant' terminal oxidase. *Functional Plant Biology* **35**: 535-552.
- McDonald AE, Vanlerberghe AE. 2006.** Origins, evolutionary history, and taxonomic distribution of alternative oxidase and plastoquinol terminal oxidase. *Comparative Biochemistry and Physiology Part D: Genomics and Proteomics* **1**: 357-364.
- Meeuse BJ. 1966.** The voodoo lily. *Scientific American* **218**: 80-88.
- Meeuse BJD. 1975.** Thermogenic respiration in aroids. *Annual Review of Plant Physiology and Plant Molecular Biology* **26**: 117-126.
- Meeuse BJD, Raskin I. 1988.** Sexual reproduction in the arum lily family, with emphasis on thermogenicity. *Sexual Plant Reproduction* **1**: 3-15.
- Miyake K. 1898.** Some physiological observations on *Nelumbo nucifera*, G. *Botanical Magazine Tokyo* **12**: 112-117.
- Nagy KA, Odell DK, Seymour RS. 1972.** Temperature regulation by the inflorescence of *Philodendron*. *Science* **178**: 1195-1197.
- Onda Y, Kato Y, Abe Y, Ito T, Ito-Inaba Y, Morohashi M, Ito Y, Ichikawa M, Otsuka M, Koiwa H, Ito K. 2007.** Pyruvate-sensitive AOX exists as a non-covalently associated dimer in the homeothermic spadix of the skunk cabbage, *Symplocarpus renifolius*. *FEBS Letters* **581**: 5852-5858.
- Onda Y, Kato Y, Abe Y, Ito T, Morohashi M, Ito Y, Ichikawa M, Matsukawa K, Kakizaki Y, Kiowa H, Ito K. 2008.** Functional coexpression of the mitochondrial alternative

- oxidase and uncoupling protein underlies thermoregulation in the thermogenic florets of skunk cabbage. *Plant Physiology* **146**: 636-645.
- Pring DR, Tang HV, Chase CD, Siripant MN. 2006.** Microspore gene expression associated with cytoplasmic male sterility and fertility restoration in sorghum. *Sexual Plant Reproduction* **19**: 25-35.
- Rhoads DM, McIntosh L. 1992.** Salicylic acid regulation of respiration in higher plants: Alternative oxidase expression. *Plant Cell* **4**(9): 1131–1139.
- Rhoads DM, Umbach AL, Sweet CR, Lennon AM, Rauch GS, Siedow JN. 1998.** Regulation of the cyanide-resistant alternative oxidase of plant mitochondria. The identification of the cysteine residue involved in  $\alpha$ -keto acid stimulation and intersubunit disulfide bond formation. *Journal of Biological Chemistry* **273**: 30750-30756.
- Ribas-Carbo M, Berry JA, Yakir D, Giles L, Robinson SA, Lennon AM, Siedow JN. 1995.** Electron partitioning between the cytochrome and alternative pathways in plant mitochondria. *Plant Physiology* **109**: 829-837.
- Ribas-Carbo M, Robinson SA, Giles L 2005.** The application of the oxygen-isotope techniques to assess respiratory pathway partitioning. In: H. Lambers, M. Ribas-Carbo eds. *Plant respiration: From cell to ecosystem. Advances in photosynthesis and respiration*. Dordrecht: Springer, 31-42.
- Seymour RS. 1991.** Analysis of heat-production in a thermogenic arum lily, *Philodendron selloum*, by 3 calorimetric methods. *Thermochimica Acta* **193**: 91-97.
- Seymour RS. 1999.** Pattern of respiration by intact inflorescences of the thermogenic arum lily *Philodendron selloum*. *Journal of Experimental Botany* **50**: 845-852.
- Seymour RS. 2001.** Diffusion pathway for oxygen into highly thermogenic florets of the arum lily *Philodendron selloum*. *Journal of Experimental Botany* **52**: 1465-1472.
- Seymour RS, Barnhart MC, Bartholomew GA. 1984.** Respiratory gas exchange during thermogenesis in *Philodendron selloum* Koch. *Planta* **161**: 229-232.
- Seymour RS, Bartholomew GA, Barnhart MC. 1983.** Respiration and heat production by the inflorescence of *Philodendron selloum* Koch. *Planta* **157**: 336-343.
- Seymour RS, Gibernau M. 2008.** Respiration of the thermogenic inflorescences of *Philodendron melinonii*: Natural pattern and responses to experimental temperatures. *Journal of Experimental Botany* **59**(6): 1353-1362.
- Seymour RS, Schultze-Motel P. 1996.** Thermoregulating lotus flowers. *Nature* **383**: 305.
- Sluse FE, Almeida AM, Jarmuszkiewicz W, Vercesi AE. 1998.** Free fatty acids regulate the uncoupling protein and alternative oxidase activities in plant mitochondria. *FEBS Letters* **433**(3): 237-240.
- Tang M, Sternberg L, Price D. 1987.** Metabolic aspects of thermogenesis in male cones of five cycad species. *American Journal of Botany* **74**: 1555-1559.
- Vanlerberghe GC, McIntosh L. 1997.** Alternative oxidase: From gene to function. *Annual Review of Plant Physiology and Plant Molecular Biology* **48**: 703-734.
- Wagner AM, Krab K, Wagner MJ, Moore AL. 2008.** Regulation of thermogenesis in flowering Araceae: The role of the alternative oxidase. *Biochimica et Biophysica Acta* **1777**(7-8): 993-1000.
- Wagner AM, Wagner MJ, Moore AL. 1998.** *In vivo* ubiquinone reduction levels during thermogenesis in Araceae. *Plant Physiology* **117**: 1501-1506.
- Walker DB, Gysi J, Sternberg L, DeNiro MJ. 1983.** Direct respiration of lipids during heat production in the inflorescence of *Philodendron selloum*. *Science* **220**: 419-421.
- Watling JR, Robinson SA, Seymour RS. 2006.** Contribution of the alternative pathway to respiration during thermogenesis in flowers of the sacred lotus, *Nelumbo nucifera*. *Plant Physiology* **140**(4): 1367-1373.
- Wilson RH, Smith BN. 1971.** Uncoupling of *Sauromatum* spadix mitochondria as a mechanism of thermogenesis. *Zeitschrift für Pflanzenphysiologie* **65**: 124-129.

### *Supporting Information*

**Figure S1.** Total respiratory flux and flux via the AOX pathway in sterile male *Philodendron bipinnatifidum* florets; respiration and discrimination were measured sequentially, first in increased oxygen, second in air, and third in increased oxygen.

### *Figure Legends*

**Figure 1.** Typical temperature traces for sterile and fertile male florets of *Philodendron bipinnatifidum* (a) *in planta* and (b) excised from the plant, and (c) photographs of inflorescences at the developmental stages (A-F). In (a) temperatures traces are means of three inflorescences logged concurrently shown relative to air temperature over the same two day period. Time is Standard Eastern Australian summer time. Letters indicate thermogenic stages: B shoulder, C peak thermogenesis, D dip, E plateau and F post-thermogenesis. N.B. Stage A pre-thermogenesis not shown. Sunrise was 05:48 and sunset was 19:38. Temperature traces of excised fertile and sterile male florets, and non-thermogenic spathe tissue recorded in the laboratory are from spadices sampled late (5pm) and early (1pm) during stage B.

**Figure 2.** (a) Total respiratory flux (grey +white) and fluxes through the AOX (white) and COX (grey) pathways by developmental stage in fertile male florets, and (b) total respiratory flux by developmental stage in sterile male (SM) florets of *Philodendron bipinnatifidum*. Diffusional limitations in SM florets prevented accurate determination of electron partitioning, thus, only total flux is shown in (b). Developmental stages: A pre-thermogenesis, B shoulder, C peak, E plateau (refer to Fig. 1a for details). Stage C/D: FM peak fluxes were not apparently captured (see Fig. 3a) and samples are likely a mix of stages C and D (dip). Letters indicate significant differences at  $P < 0.05$ . Data are means  $\pm$  SE of  $n=4-7$  samples.

**Figure 3.** Relationships between total respiratory flux and heating in (a) FM florets and (b) SM florets, and between AOX (solid circles) and COX flux (open triangles) and floret heating in (c) fertile male florets and (d) sterile male florets. Heating was measured as the difference in temperature between FM florets ( $T_{mf}$ ) or SM florets ( $T_{smf}$ ), and adjacent non-thermogenic spathe tissue ( $T_{sp}$ ). Peak thermogenic stage C FM florets were excluded from correlations for

both (a); total respiration (open circles) and (c); AOX (open circles) and COX fluxes (closed triangles). The regression equations are included in the text. Correlations between COX and AOX fluxes and heating not shown for SM florets due to potential diffusional limitation of isotope fractionation in air.

**Figure 4.** Theoretical discrimination (Dt; lines) as a function of external O<sub>2</sub> (%) determined from equation 2 and using Dr=27.1 (discrimination endpoint for AOX measured under elevated O<sub>2</sub>). Pi/Pa was calculated using  $P_i/P_a=(P_a-G)/P_a$ , where G is the diffusion gradient, which was assumed to remain constant as there was no change in respiration rate as O<sub>2</sub> was increased above 21%, as shown by the relative flux rates (closed circles) which vary little from 1 (horizontal line; mean  $\pm$  SD,  $1.0 \pm 0.05$ ). Dt response curves are shown for diffusion gradients (G) of 5.0% (solid line), 7.5% (dashed line) or 10% (dotted line). Using G=7.5% gave the best fit for the actual isotopic discrimination data (Dt) for stage C SM florets (open triangles). For Dt measurements,  $n=15$  floret samples from 5 inflorescences.

**Figure 5.** Densitometry results of chemiluminescent signals from western blots of AOX (a, b, d), COXII (d, e, f) and pUCP (g, h, i) proteins presented relative to Porin in fertile male florets (left panels), sterile male florets (centre panels) and female florets (right panels) of *Philodendron bipinnatifidum* during development. Developmental stages: A pre-thermogenesis, B shoulder, C peak, E plateau, F post-thermogenesis (refer to Fig. 1a for details). Different letters indicate significant differences between stages at  $P<0.05$ . Data are means  $\pm$  SE of  $n=3-6$  samples.

**Figure 6.** Changes in total triacylglyceride content (a, b), and starch content (c, d) in fertile (left panels) and sterile (right panels) male florets of *Philodendron bipinnatifidum* during development. Developmental stages: A pre-thermogenesis, B shoulder, C peak, E plateau, F



post-thermogenesis (refer to Fig. 1a for details). Different letters indicate significant differences between stages at  $P < 0.05$ . Data are means  $\pm$  SE of  $n=4-6$  samples.

**Table I.** Mean floret temperature ( $\pm$  SD,  $n=7-14$ ) and range of heating\* for fertile male (FM) and sterile male (SM) florets of attached inflorescences of *P. bipinnatifidum* during development.

		Pre-thermogenic Stage A	Shoulder Stage B	Peak Stage C	Dip Stage D	Plateau Stage E
FM	Temperature ( $^{\circ}$ C)	$25.8 \pm 6.6$	$30.3 \pm 2.7$	$35.7 \pm 1.4^a$	$22.9 \pm 2.5$	$29.0 \pm 1.6$
Florets	Range ( $^{\circ}$ C)	0.3-2.8	1.2-9.7	5.1-21.0	2.5-8.5	2.0-11.1
SM	Temperature ( $^{\circ}$ C)	$24.4 \pm 7.3$	$30.7 \pm 1.6$	$40.1 \pm 1.4^b$	$22.5 \pm 1.9$	$28.8 \pm 2.2$
Florets	Range ( $^{\circ}$ C)	0-3.2	2.7-10.6	8.1-26.5	3.5-7.0	1.3-13.9

\*Heating was calculated as the difference between floret temperature and temperature of the non-thermogenic spathe tissue.

<sup>a,b</sup> letters indicate a significant difference in peak temperatures between FM and SM florets ( $t_{26,0}=8.19$ ,  $P<0.0001$ ), no significant differences were found for the other developmental stages.

**Table II.** Mean proportion and range (%) of total respiratory flux via the alternative pathway (AOX) in *Philodendron bipinnatifidum* sterile male florets during stages C and E, measured in air ( $n=4-5$ ) and in on average 55% O<sub>2</sub> ( $n=3-4$ ).

	Mean proportion of flux via AOX (% ± SE)	Range of flux via AOX (%)	Mean proportion of flux via AOX (% ± SE)	Range of flux via AOX (%)
Stage	Measured in air		Measured in ~55% O <sub>2</sub>	
Peak (C)	15.7 ± 4.5	6.7 - 28.0	70.8 ± 2.5	52.3 – 95.5
Plateau (E)	28.9 ± 12.2	0 - 59.6	63.3 ± 5.2	42.0 – 87.5

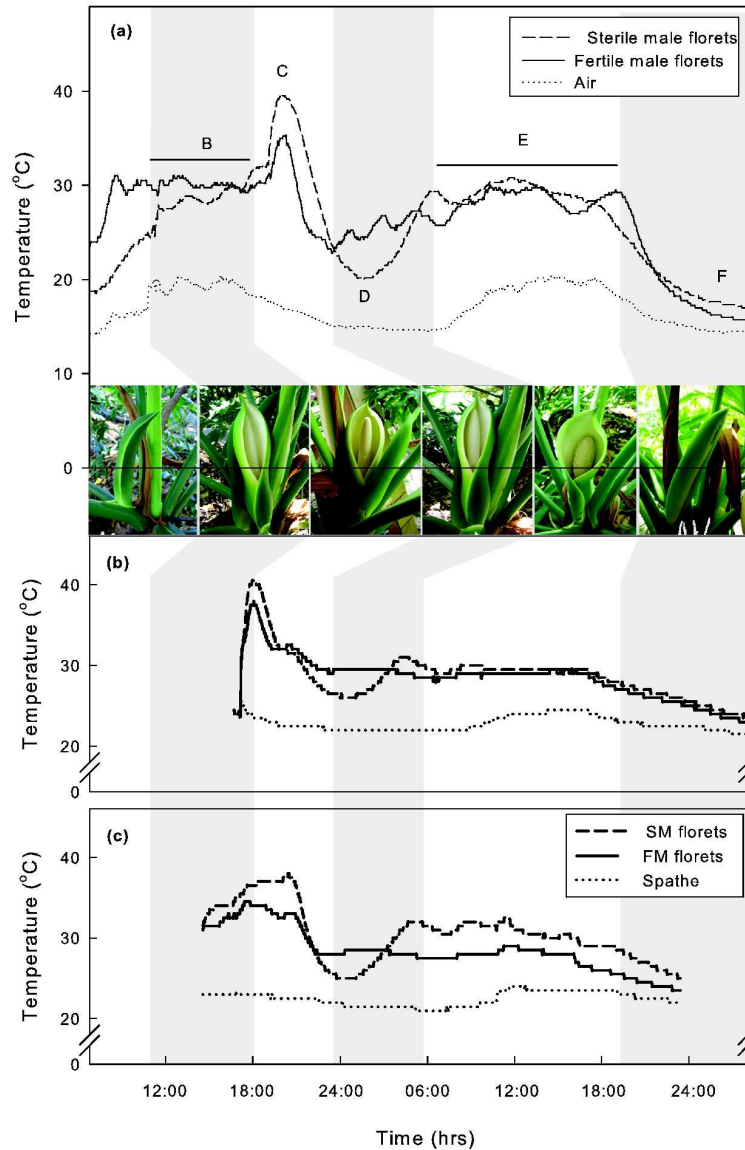


Figure 1. Typical temperature traces for sterile and fertile male florets of *Philodendron bipinnatifidum* (a) in planta and (b) excised from the plant, and (c) photographs of inflorescences at the developmental stages (A-F). In (a) temperatures traces are means of three inflorescences logged concurrently shown relative to air temperature over the same two day period. Time is Standard Eastern Australian summer time. Letters indicate thermogenic stages: B shoulder, C peak thermogenesis, D dip, E plateau and F post-thermogenesis. N.B. Stage A pre-thermogenesis not shown. Sunrise was 05:48 and sunset was 19:38. Temperature traces of excised fertile and sterile male florets, and non-thermogenic spathe tissue recorded in the laboratory are from spadices sampled late (5pm) and early (1pm) during stage B.

176x251mm (600 x 600 DPI)

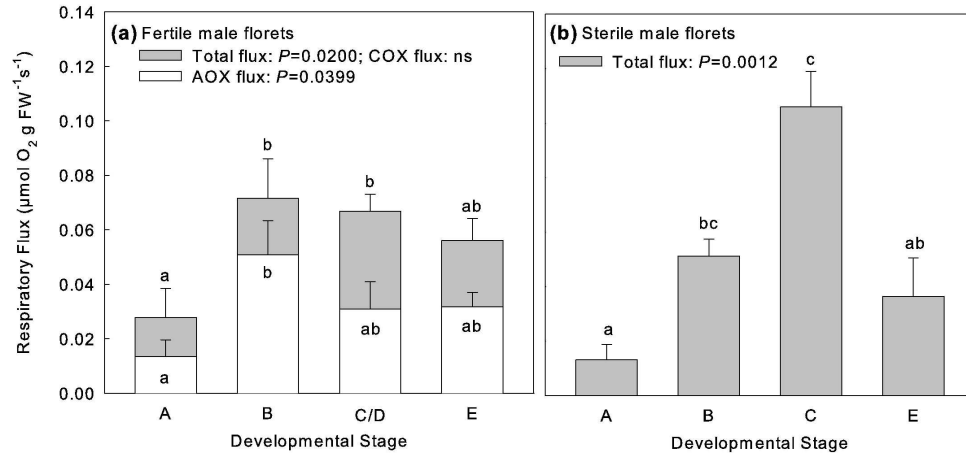


Figure 2. (a) Total respiratory flux (grey +white) and fluxes through the AOX (white) and COX (grey) pathways by developmental stage in fertile male florets, and (b) total respiratory flux by developmental stage in sterile male (SM) florets of *Philodendron bipinnatifidum*. Diffusional limitations in SM florets prevented accurate determination of electron partitioning, thus, only total flux is shown in (b). Developmental stages: A pre-thermogenesis, B shoulder, C peak, E plateau (refer to Fig. 1a for details). Stage C/D: FM peak fluxes were not apparently captured (see Fig. 3a) and samples are likely a mix of stages C and D (dip). Letters indicate significant differences at  $P < 0.05$ . Data are means  $\pm$  SE of  $n=4-7$  samples.

189x128mm (600 x 600 DPI)

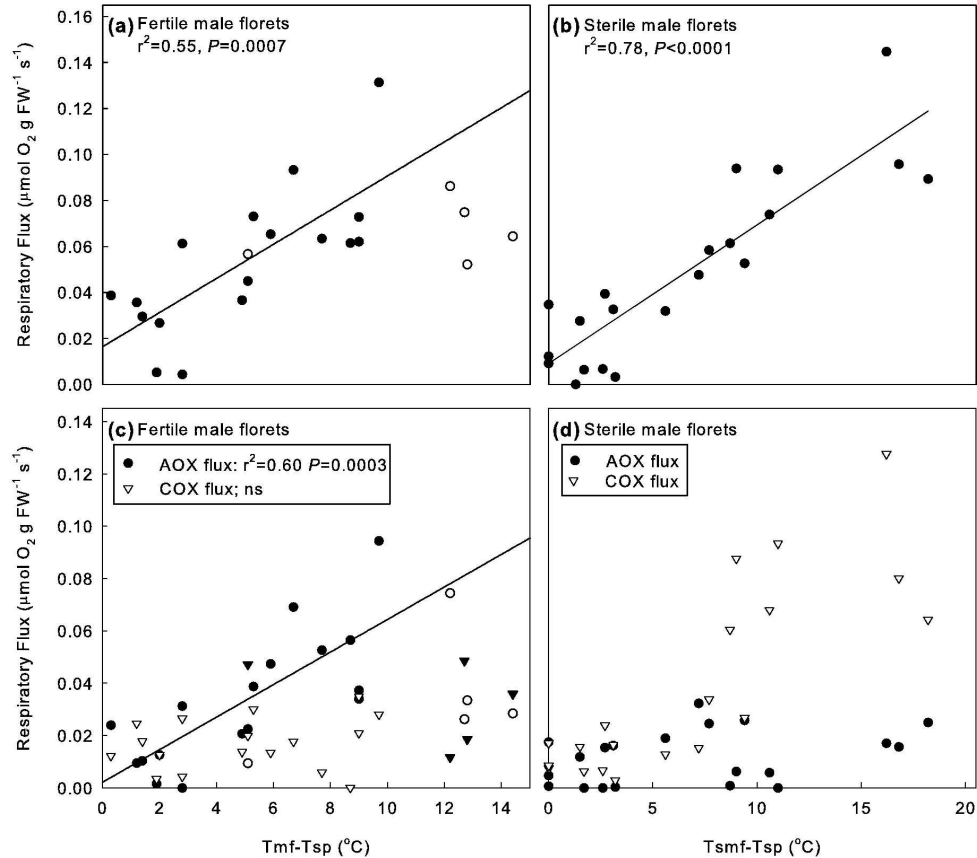


Figure 3. Relationships between total respiratory flux and heating in (a) FM florets and (b) SM florets, and between AOX (solid circles) and COX flux (open triangles) and floret heating in (c) fertile male florets and (d) sterile male florets. Heating was measured as the difference in temperature between FM florets (Tmf) or SM florets (Tsmf), and adjacent non-thermogenic spathe tissue (Tsp). Peak thermogenic stage C FM florets were excluded from correlations for both (a); total respiration (open circles) and (c); AOX (open circles) and COX fluxes (closed triangles). The regression equations are included in the text. Correlations between COX and AOX fluxes and heating not shown for SM florets due to potential diffusional limitation of isotope fractionation in air. 159x147mm (600 x 600 DPI)

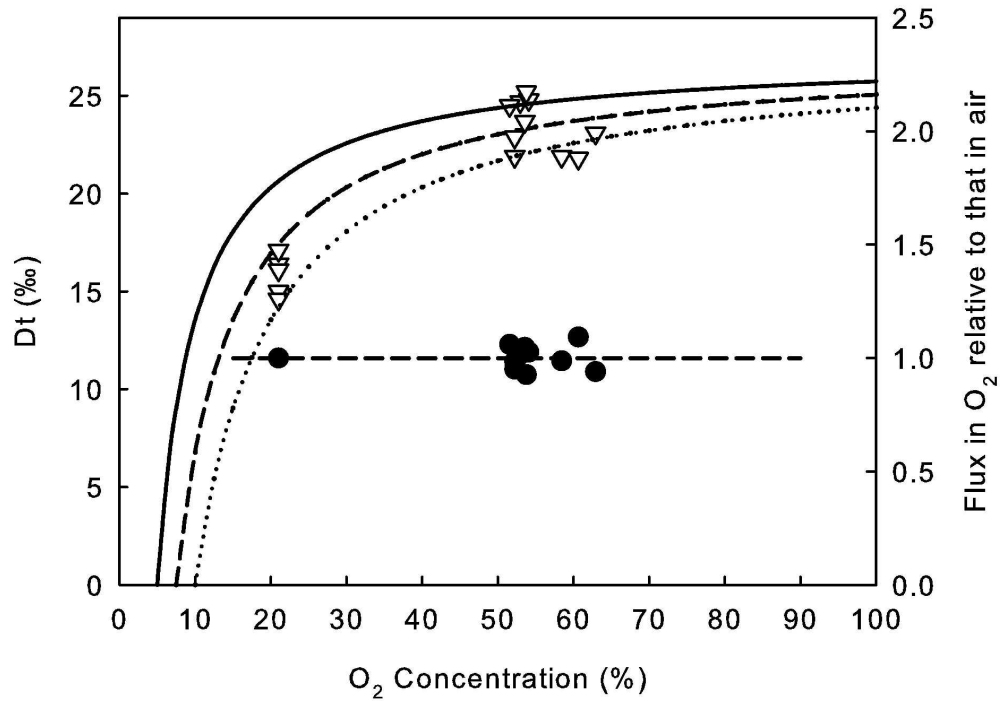


Figure 4. Theoretical discrimination ( $D_t$ ; lines) as a function of external  $O_2$  (%) determined from equation 2 and using  $D_r=27.1$  (discrimination endpoint for AOX measured under elevated  $O_2$ ).  $P_i/P_a$  was calculated using  $P_i/P_a=(P_a-G)/P_a$ , where  $G$  is the diffusion gradient, which was assumed to remain constant as there was no change in respiration rate as  $O_2$  was increased above 21%, as shown by the relative flux rates (closed circles) which vary little from 1 (horizontal line; mean  $\pm$  SD,  $1.0 \pm 0.05$ ).  $D_t$  response curves are shown for diffusion gradients ( $G$ ) of 5.0% (solid line), 7.5% (dashed line) or 10% (dotted line). Using  $G=7.5\%$  gave the best fit for the actual isotopic discrimination data ( $D_t$ ) for stage C SM florets (open triangles). For  $D_t$  measurements,  $n=15$  floret samples from 5 inflorescences.  
159x125mm (600 x 600 DPI)

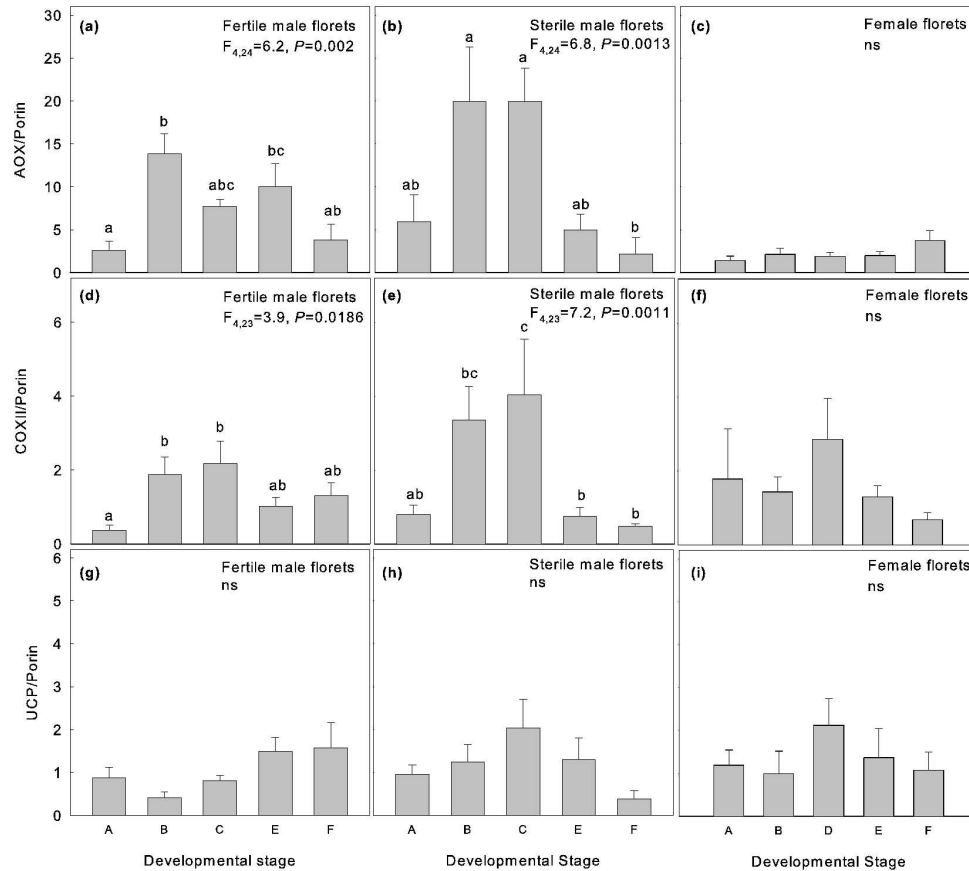


Figure 5. Densitometry results of chemiluminescent signals from western blots of AOX (a, b, d), COXII (d, e, f) and pUCP (g, h, i) proteins presented relative to Porin in fertile male florets (left panels), sterile male florets (centre panels) and female florets (right panels) of *Philodendron bipinnatifidum* during development. Developmental stages: A pre-thermogenesis, B shoulder, C peak, E plateau, F post-thermogenesis (refer to Fig. 1a for details). Different letters indicate significant differences between stages at  $P < 0.05$ . Data are means  $\pm$  SE of  $n=3-6$  samples. 216x200mm (600 x 600 DPI)



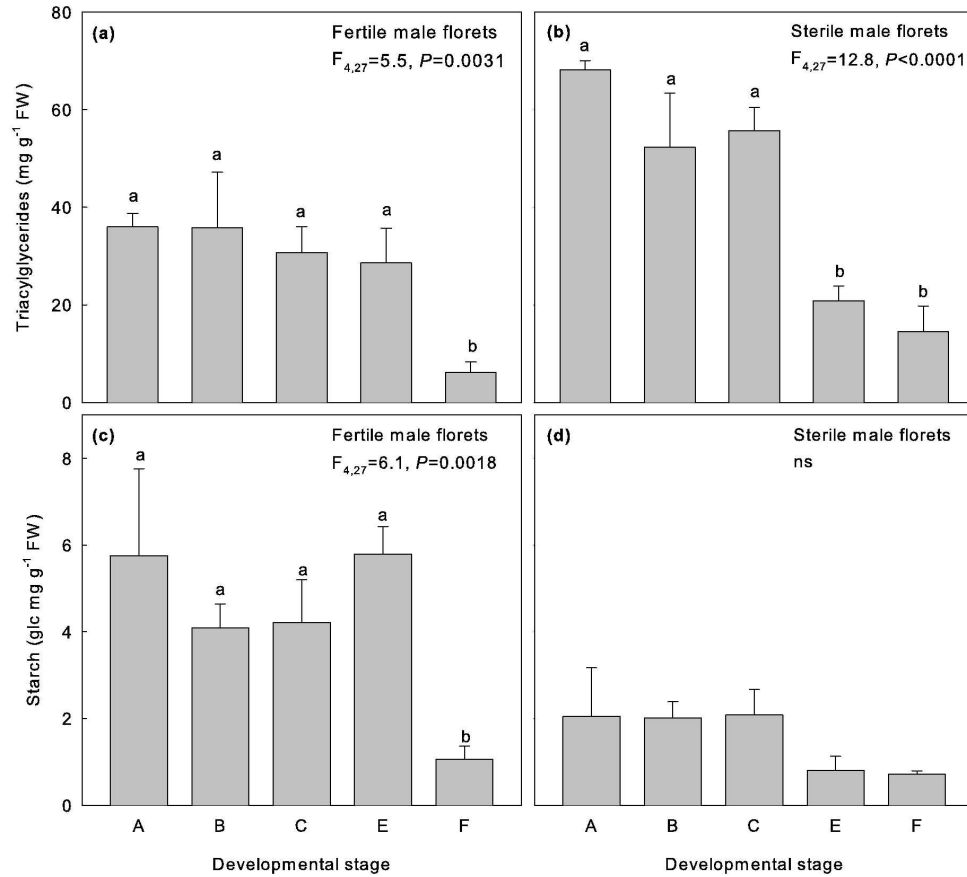


Figure 6. Changes in total triacylglyceride content (a, b), and starch content (c, d) in fertile (left panels) and sterile (right panels) male florets of *Philodendron bipinnatifidum* during development. Developmental stages: A pre-thermogenesis, B shoulder, C peak, E plateau, F post-thermogenesis (refer to Fig. 1a for details). Different letters indicate significant differences between stages at  $P<0.05$ . Data are means  $\pm$  SE of  $n=4-6$  samples.  
159x143mm (600 x 600 DPI)